



ARTICLE

The design basis for the integrated and continuous biomanufacturing framework

Jon Coffman¹  | Kenneth Bibbo² | Mark Brower³ | Robert Forbes² |
 Nicholas Guros¹ | Brian Horowski² | Rick Lu⁴ | Rajiv Mahajan⁴ |
 Ujwal Patil¹  | Steven Rose¹ | Joseph Shultz⁵

¹Biopharmaceutical Development, R&D, AstraZeneca, Gaithersburg, Maryland, USA

²US Lifescience, Wood PLC, Philadelphia, Pennsylvania, USA

³Merck and Co., Inc., Kenilworth, New Jersey, USA

⁴Operations Management, Supply Biologics, AstraZeneca, Gaithersburg, Maryland, USA

⁵Novartis, Basel, Switzerland

Correspondence

Jon Coffman, Biopharmaceutical Development, R&D, AstraZeneca, Gaithersburg 20878, MD, USA.
 Email: drcoffman@gmail.com

Abstract

An 8 ton per year manufacturing facility is described based on the framework for integrated and continuous bioprocessing (ICB) common to all known biopharmaceutical implementations. While the output of this plant rivals some of the largest fed-batch plants in the world, the equipment inside the plant is relatively small: the plant consists of four 2000 L single-use bioreactors and has a maximum flow rate of 13 L/min. The equipment and facility for the ICB framework is described in sufficient detail to allow biopharmaceutical companies, vendors, contract manufacturers to build or buy their own systems. The design will allow the creation of a global ICB ecosystem that will transform biopharmaceutical manufacturing. The design is fully backward compatible with legacy fed-batch processes. A clinical production scale is described that can produce smaller batch sizes with the same equipment as that used at the commercial scale. The design described allows the production of as little as 10 g to nearly 35 kg of drug substance per day.

KEYWORDS

biopharmaceutical, dual-column chromatography, integrated continuous bioprocessing, mammalian cells, perfusion, protein therapeutics

1 | INTRODUCTION

Many biopharmaceutical companies are investigating the next generation of biologics manufacturing by developing integrated and continuous bioprocessing (ICB). As shown in the companion article, a common framework for ICB exists that would enable ICB processes currently being implemented. It can be implemented in a staged approach, allowing the deferral of capital investment, labor hiring, and consumable purchases until increased productivity is required. While this process is being implemented at AstraZeneca, we believe that the design described here will benefit

biopharmaceutical companies and contract manufacturing companies implement ICB, and provide the process description in sufficient detail to enable plug-and-play equipment supporting the common ICB framework.

The plant and equipment designs described here can produce quantities of recombinant proteins that would satisfy any market need. Very few products require over 1 ton of material per year (Kelley, 2009); the framework design is capable of 8 ton per year.

The world has an urgent need for quickly expandable manufacturing space which may require 8 ton per year. Due to the COVID-19 pandemic, many companies are buying up existing capacity in large stainless-steel

This is an open access article under the terms of the Creative Commons Attribution-NonCommercial License, which permits use, distribution and reproduction in any medium, provided the original work is properly cited and is not used for commercial purposes.

© 2021 The Authors. *Biotechnology and Bioengineering* Published by Wiley Periodicals LLC

facilities for their antibody treatments. Expanding these facilities will take about five years. In addition, these facilities cost \$400–800 M (Jagschies, 2020). Finally, due to supply chain concerns, many countries and regions want to manufacture these COVID-19 treatments within their political sphere of influence (Hafner et al., 2020).

The common framework enables single-use equipment to be as productive as larger stainless-steel plants. By enabling cost-effective use of single-use technologies, the common framework allows the fast, and relatively inexpensive, building of large-capacity biomanufacturing in nearly any locality.

Examples are provided that include a 500 L bioreactor with a low productivity cell line and 2000 L bioreactors with a high productivity cell line. The 500 L bioreactor makes about 0.5 kg of material in the bioreactor per day, which results after 20 days in a 6 kg batch. The 2000 L bioreactor makes about 10 kg of material per day, which results after 20 days in a 120 kg batch. A four 2000 L process is described that results in as much as a 500 kg batch over 20 days, or about 8 ton per year in 17 batches. These upstream options are integrated with a downstream design that is flexible enough to allow an almost 10,000-fold productivity range.

2 | MATERIALS AND METHODS

The design of the upstream and downstream was based on common and well-known engineering principles. The design examples are shown in Table 1. The justification for the design, and a more detailed materials and methods, is in the Supporting Information. In addition, a spreadsheet is enclosed in the Supporting Information that can enable other manufacturing scenarios. A spreadsheet is located online, which will allow further development of new technologies (Coffman, 2020).

3 | RESULTS AND DISCUSSION

The high-level consequences of the common framework ICB are discussed in the accompanying article (Coffman et al., 2020). Here we discuss the details of the design to demonstrate the flexibility and productivity of the framework ICB. The examples used are shown in Figure 1 and Tables 1 and 2. They are described in more detail below.

3.1 | Bioreactor design

The common framework bioreactor is designed to support high cell densities. The largest design challenges deal with supplying cells with O_2 and stripping cells of CO_2 . The mass of nutrients required by high cell densities requires the development of media concentrates, as well as the possibility of several feed solutions. The high density of cells also requires cooling to maintain the temperature. While these challenges impact the bioreactor design in several ways, they do not preclude the bioreactor for standard fed-batch operation.

Dynamic, or non-steady-state perfusion, where the cell density is not directly controlled by a bleed, can reach cell densities of 100–150 Mcells/ml (Wolf et al., 2020). These cell densities would require oxygen transfer rates between 15 and 50 mM/h, as shown in Table 2 (Jorjani & Ozturk, 1999). The gas/liquid transfer coefficient $k_L a$ between 15 and 70 h^{-1} would be required (Moutafchieva et al., 2013). The cells consume oxygen so fast that they become hypoxic in less than 10 s without sparging (see supplemental information). Further, there are a few lab or pilot scale examples of perfusion cell culture at 240 M cells/ml (Clincke, Molleryd, Samani, et al., 2013; Clincke, Molleryd, Zhang, et al., 2013; Zamani et al., 2018). If the industry is to expand to this cell density, a $k_L a$ of over 100 h^{-1} , or lower cell-specific oxygen uptake rates, would be required.

The gassing strategy for a perfusion culture is a three-fold balancing act between control of dissolved oxygen (DO), pCO_2 accumulation (i.e., pH and subsequent base utilization), and foam formation. Achieving desired control in any one aspect can result in an undesirable result in another aspect.

The supply of oxygen to the cells can easily be the limiting factor in achieving high cell densities (Ozturk, 1996; Zhu et al., 2017). The design of the mass-flow controller and sparger require consideration. Generally, mass-flow controllers delivering air and O_2 for perfusion processes requires significantly higher flow capacity than fed-batch processes, ranging from 0.05vvm to 0.2vvm. With respect to sparger design, micro-spargers have been demonstrated to improve the oxygen transport capacity needed to achieve a desired DO at perfusion-scale cell densities (Diekmann et al., 2011; Dreher et al., 2014). However, microspargers raise several concerns, including their potential to cause cell damage due to shear when the microscopic bubbles burst (Wolf et al., 2020). Microspargers have also been observed to yield higher pCO_2 accumulation than traditional macro, i.e. ring or drilled-hole, spargers (Dreher et al., 2014), which lowers culture pH, and increases base utilization, which can be increase cell stress and the rate of cellular apoptosis. Additionally, microsparging creates a thicker layer of foam than traditional spargers. This thick foam requires enhanced control methods, and is a concern with respect to fouling bioreactor exhaust.

A dual-sparger design that is composed of a microsparger and a macrosparger permits the most flexibility in configuring the gas flows to balance the requirements for dissolved oxygen, dissolved carbon dioxide, and foam management in a perfusion bioreactor. In this design, the microsparger component generally provides the required dissolved oxygen to a culture via relatively smaller bubbles and the macrosparger component generally provides a means to manage pCO_2 accumulation via stripping carbon dioxide from the system with relatively larger air bubbles. The dual-sparger design can also provide an additional benefit of reducing the amount of foam generated via destruction interactions between the two bubble sizes (Karakashev et al., 2012).

Even with a dual sparger design, foam and aerosol management is more difficult in perfusion cultures due to relatively higher agitation and gas flow rates than fed-batch cultures. The first line of defense is to manage foam generation in the bioreactor itself through means such as mechanical disturbance, adjustment of overlay humidity, and

TABLE 1 Design examples for the common framework integrated and continuous bioprocess

| Parameter | Clinical production | 2000L, MCC High cellular productivity | 4 × 2000 L high productivity |
|---|---------------------|---------------------------------------|------------------------------|
| Bioreactor | | | |
| Bioreactor size (L) | 500 | 2000 | 8000 |
| Avg cell density (M cells/ml) | 50 | 120 | 120 |
| Qp (ng/cell/day) | 20 | 40 | 40 |
| O ₂ (VVM) | 0.2 | 0.2 | 0.2 |
| Air (VVM) | 0.2 | 0.2 | 0.2 |
| Perfusion rate (permeate) vvd | 1.5 | 1.5 | 1.5 |
| Batch duration (days) | 20 | 20 | 20 |
| Media concentration factor, average | 3 | 3 | 3 |
| Media components, liquid | 5 | 5 | 5 |
| Cell retention | | | |
| Membrane capacity (L/m ²) | 1000 | 1000 | 1000 |
| Yield | 90% | 90% | 90% |
| Number of membrane sets per run | 2 | 2 | 8 |
| Number of modules in series | 2 | 4 | 4 |
| Capture | | | |
| Linear flowrate (cm/h) | 300 | 300 | 300 |
| Bed height (cm) | 20 | 10 | 10 |
| Capacity (g/L) | 60 | 72 | 72 |
| # Columns | 2 | 2 | 2 |
| Total cycles/day | 10 | 20 | 20 |
| Yield | 95% | 95% | 95% |
| Virus inactivation | | | |
| Acid ratio addition (L acid/L peak pool) | 10% | 10% | 10% |
| Base ratio addition (L base/L acid) | 100% | 100% | 100% |
| Yield | 98% | 98% | 98% |
| Depth filtration capacity (L/m ²) | 200 | 200 | 200 |
| Polishing Step 1: Flow thru | | | |
| Bed height (cm) | 20 | 10 | 10 |
| Capacity (g/L) | 100 | 120 | 120 |
| # Columns | 2 | 2 | 2 |
| Cycles per day | 1 | 18 | 25 |
| Yield | 95% | 95% | 95% |

(Continues)

TABLE 1 (Continued)

| Parameter | Clinical production | 2000L, MCC High cellular productivity | 4 × 2000 L high productivity |
|---------------------------------------|---------------------|---------------------------------------|------------------------------|
| Polishing Step 2: Bind and elute | | | |
| Capacity (g/L) | 40 | 48 | 48 |
| # Columns | 2 | 2 | 2 |
| Total cycles per day | 1 | 20 | 25 |
| Yield | 85% | 85% | 85% |
| Elution volume per cycle (cv) | 1.2 | 1.2 | 1.2 |
| Virus filtration | | | |
| Capacity (L/m ²) | 700 | 700 | 700 |
| Flux (LMH) | 100 | 100 | 100 |
| Number of sub-batches | 1 | 20 | 20 |
| Yield | 95% | 95% | 95% |
| Batch UDFD option | | | |
| Membrane capacity (L/m ²) | 1000 | 1000 | 1000 |
| Yield | 95% | 95% | 95% |
| Cross flow (LMH) | 390 | 390 | 390 |
| Concentration 1 flux (LMH) | 45 | 45 | 45 |
| Concentration 1 target (g/L) | 50 | 50 | 50 |
| # Diavolumes (L/L) | 6 | 6 | 6 |
| Final concentration target (g/L) | 150 | 150 | 150 |
| Final DS conc target (g/L) | 100 | 100 | 100 |
| SPTFF-UF option | | | |
| Feed product concentration (g/L) | 26 | 32 | 32 |
| Feed flow (L/h) | 10.1 | 8.0 | 31.9 |
| SPTFF UF target (g/L) | 150 | 150 | 150 |
| Filtration flux (LMH) | 15 | 15 | 15 |
| Number of stages | 3 | 3 | 3 |
| Final DS conc target (g/L) | 150 | 150 | 150 |

automated addition of antifoaming agents as a function of the rate of foam generation and foam thickness (Proulx et al., 2019). Redundant filters and/or vent traps are essential components of the exhaust manifold to manage the collection of foam and aerosols, as is the ability to seamlessly switch between such unit operations while maintaining a sterile boundary. Advanced filtration systems (Le Merdy et al., 2017; Pegel et al., 2011) demonstrate an enhanced ability to manage foam and aerosol generation, and should be considered for implementation in any bioreactor exhaust manifold.

The last consideration for the perfusion bioreactor gassing strategy is the control strategy. Essential to maintaining the balance

between DO, pCO₂ accumulation, and foam generation is establishing bioreactor-specific relationships for the parameters that govern this balance, including the gas transfer (i.e., $k_L a$) for a given gas species and sparger design. Therefore, it is essential for perfusion bioreactor control architecture to permit the use of reasonably complex algorithms (Abbate et al., 2020) to manage these three control elements, as well as the ability to incorporate so-called off-line, at-line, and online measurements such as cell density, temperature, lactic acid concentration, glucose concentration, and pH.

Media delivery is also different for high-cell density perfusion compared to fed-batch. The media is concentrated and can be in

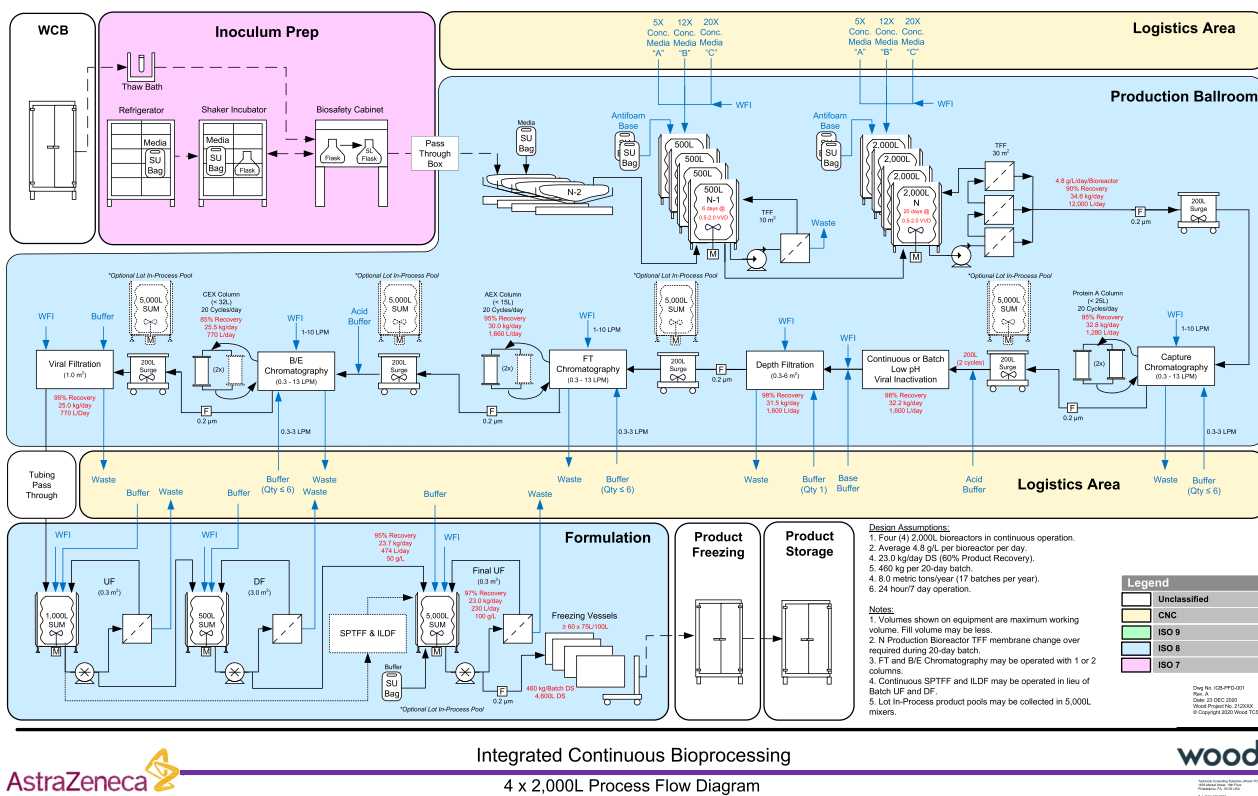


FIGURE 1 The common framework for integrated and continuous bioprocessing, showing the process flow from seed vial through to drug substance

multiple streams rather than one stream. In the scenarios shown in Table 1, the media concentrates are made up of a $\times 5$, $\times 12$, and $\times 20$ concentrates, which, taken as a whole, are effectively $\times 3$ concentrate. Multiple media feed pumps sized from 0.02 vvd to 0.3vvd would be needed. For a 2000 L bioreactor, this is a surprisingly small 20–400 ml/min. A glucose concentrate and antifoam will also need to be added with even smaller flow rates. The pump rates should be capable of being set by complicated calculations that may rely on PAT or on mechanistic models, similar to the ones that might be required for gassing. Overall bioreactor level control is required to control the feeds or the permeate rate.

The media concentrates may be added through a single line with a static mixer. Typically, a line of water enters the static mixer, and a series of T-connections allow the mixing of each concentrate in a serial fashion.

The use of media concentrates greatly reduces the size of the media preparation and media storage area. In the 4×2000 L scenario shown in Tables 1 and 2, the media can be stored in sixteen 5000 L single use containers. The $\times 20$ media would require an additional 2000 L container.

These bioreactors may become exothermic and require cooling due to the exceptional quantity of cell mass, a novel concern for perfusion as compared to batch mammalian cell culture. Cells generate about 28 pW/cell (Kemp & Guan, 1997) or between 1.4 and 4.2 W/L for cell densities between 50 and 150 Mcells/ml. A 2000 L vessel could generate 3000 and

8000 W, which is easily handled by modifying the heating jacket to allow cooling as well. Cooling a 12 kL bioreactor may, however, become a limitation as the cells could generate up to 50 kW. A heat exchanger in line with the tangential flow filtration system may become necessary.

A design that might be suitable for a clinical manufacturing facility is shown in Column 1 in Tables 1 and 2. The 500 L bioreactor operates at 50 Mcell/ml with a 20 pg/cell/day cell line. This scenario represents one that can be achieved by converting a fed-batch process to perfusion cell-culture without much difficulty. It also represents one that might occur early in development, when process optimization and intensification has not occurred. The bioreactor makes 500 g/day.

A commercial bioreactor set up is shown in Tables 1 and 2, and column 3, operating at an average cell density of 120 Mcell/ml with a 40pcd cell line. In this scenario, four 2000 L bioreactors are operated to feed a single downstream. The bioreactors together produce on average 38 kg per day. Over the course of the 20-day run, over 500 kg of material is pooled into a single lot.

3.2 | Cell retention design

The common framework bioreactor supports both ATF and TFF operation. The TFF and ATF design is shown in Tables 1 and 2 for a 500 and 2000 L bioreactor. To mitigate against Starling flow

TABLE 2 The assumptions in Table 1 result in a design basis for the framework integrated and continuous bioprocessing plant, summarized here

| | | | |
|--|--------|---------|---------|
| Bioreactor | | | |
| OUR (mM/h, approx.) | 15 | 36 | 36 |
| KLa (h ⁻¹) | 24 | 57 | 57 |
| Heat generated (Watt) | 700 | 6720 | 26,880 |
| Productivity (g/L bioreactor/day) | 1.0 | 4.8 | 4.8 |
| Bleed (ml/min) | 0 | 0 | 0 |
| Mass/day (g/day) | 500 | 9600 | 38,400 |
| Total perfusion volume (L) | 15,000 | 60,000 | 240,000 |
| Volume of 20-fold concentrate (L) | 750 | 3000 | 12,000 |
| Volume of 12-fold concentrate (L) | 1250 | 5000 | 20,000 |
| Volume of 5-fold concentrate (L) | 3000 | 12,000 | 48,000 |
| Volume total WFI for media dilution (L) | 10,000 | 40,000 | 160,000 |
| Cell retention | | | |
| Membrane area in process | 7.50 | 30.00 | 30.00 |
| Number of ATF 10 units required | 1 | 3 | 3 |
| Crossflow rate (L/min) | 70 | 68 | 68 |
| Cell residence time (s) | 2 | 7 | 7 |
| Capture | | | |
| Column volume, each (L) | 2.1 | 6.0 | 24.0 |
| Minimum column diameter (cm) | 6.5 | 15.6 | 20.0 |
| Total elution pool per day (L) | 41.7 | 240.0 | 960.0 |
| Concentrated buffer volume per day (L) | 91.7 | 528.0 | 2112.0 |
| Process flowrate for conc buffer (L/min) | 0.104 | 0.60 | 2.40 |
| Process flowrate for WFI (L/min) | 0.42 | 2.40 | 9.60 |
| Concentrated buffer volume per batch (L) | 1833 | 10,560 | 42,240 |
| Virus inactivation | | | |
| Tank volume with 20% excess | 60 | 346 | 1382 |
| Depth filter changes per batch | 20 | 20 | 20 |
| Depth filter area in process | 0.25 | 1.44 | 5.76 |
| Polishing Step 1: Flow thru | | | |
| Column volume, each (L) | 4.2 | 3.7 | 10.7 |
| Total collection pool per batch | 1017 | 6028 | 24,113 |
| Process flowrate for conc buffer | 0.2095 | 0.3724 | 0.8938 |
| Process flowrate for WFI | 0.8379 | 1.4896 | 4.4688 |
| Concentrated buffer volume per batch | 268 | 4290 | 14,300 |
| Polishing Step 2: Bind and elute | | | |
| Column volume, each (L) | 10.0 | 8.0 | 25.5 |
| Process flowrate for conc buffer (L/min) | 0.50 | 0.80 | 2.55 |
| Process flowrate for WFI (L/min) | 1.99 | 3.18 | 10.19 |
| Concentrated buffer volume per batch (L) | 738 | 10,792 | 54,017 |
| Virus filtration | | | |
| Membrane area used for processing (m ²) | 0.51 | 0.51 | 1.53 |
| Process flowrate for conc buffer (L/min) | 0.17 | 0.17 | 0.43 |
| Process flowrate for WFI (L/min) | 0.68 | 0.68 | 2.13 |
| Final pool product concentration (mg/ml) | 26 | 32 | 32 |
| Concentrated buffer volume per batch (L) | 15 | 306 | 765 |
| Total pool per batch if pooled (L) | 243 | 3828 | 15,301 |
| Batch UDFD option | | | |
| Conc 1 cross flow rate (L/min) | 0.75 | 0.45 | 1.78 |
| Diafiltration membrane area required (m ²) | 0.8 | 0.7 | 3.0 |
| Diafiltration cross flow (L/min) | 5.1 | 4.9 | 19.4 |
| Diafiltration buffer volume per batch (L) | 771 | 14,810 | 59,238 |
| Diafiltration flow rate (L/min) | 0.6 | 0.6 | 2.2 |
| Final concentration product volume per sub-batch (L) | 43 | 41 | 165 |
| Final concentration membrane area required (m ²) | 0.087 | 0.083 | 0.332 |
| Product mass per batch (g) | 6106 | 117,242 | 468,968 |
| DS product volume per batch (L) | 61 | 1172 | 4690 |
| Process flowrate (L/min) | 0.06 | 0.05 | 0.22 |
| Tank size (Conc1) with 20% excess (L) | 154.3 | 148.1 | 592.4 |
| Final pooled DS volume (L) | 61 | 1172 | 4690 |
| SPTFF-UF and CC-DF cascade | | | |
| SPTFF-UF option | | | |
| Membrane area used with 20% excess (m ²) | 1.0 | 0.8 | 3.0 |
| Retentate flow (L/H) | 1.8 | 1.7 | 6.9 |
| CC-DF three-stage cascade after SPTFF | | | |
| Feed flow (L/H) | 1.8 | 1.7 | 6.9 |
| DF buffer flow (L/H) | 19.6 | 18.9 | 75.4 |

| | | | |
|--|------|------|------|
| Flow for the diluted product stream (L/H) | 21.4 | 20.6 | 82.3 |
| Membrane area used with 20% excess (m ²) | 1.6 | 1.5 | 6.0 |
| Retentate flow (L/H) at each stage | 1.8 | 1.7 | 6.9 |
| DS product volume per batch (L) | 39 | 743 | 2970 |

(Radoniqi et al., 2018), the membrane area was scaled up by adding filter modules in series, rather than in parallel. The 2000 L bioreactor requires four hollow fiber modules in series (see Figure 1, TFF step). A parallel scale-up strategy would require the retentate flow rate to be between 500 and 1000 L/min, or 0.25–0.5 vvm. These flow rates would require very large pumps, and the cells would have 5–10 times more pump passes. Damage to cells through pumps is an important factor to mitigate (Wang et al., 2017).

Switching the filter for the 2000 L bioreactor design is best accomplished by the use of Y-connectors and valves between the two sets of filter modules. Ideally, the connectors would have zero dead volume, so cells do not get stuck in the dead leg. Manual switching between the two sets of filter modules is likely acceptable for most operations, even in commercial space.

The design optionally allows for one ATF10 systems for the 500 L bioreactor and three per 2000 L bioreactor. While this takes up a considerable amount of floor space around the bioreactor, it is not a major inconvenience.

The area required for both ATF and TFF on the 2000 L bioreactor is 30 m². Modules are commercially available. The ATF and TFF systems require three or four small permeate pumps with a maximum flow rate of less than 1 L/min. The total flow rate onto the capture step is small, about 8 L/min for the 4 × 2000 L design. It should be noted that the residence time of the cells in either the ATF or TFF filters is near the time to hypoxia.

Single-use bioreactors over 500 L do well to have 1.5- to 2-in. ports to allow unrestricted flow for each pump system. Connecting the SUB to the TFF requires a 1.5-in. sanitary connection, which is not known to be commercially available. Instead, two 1-in. ports are often used for each connection. This arrangement is suboptimal. The 2000 L bioreactor requires four 1.5- to 2-in. ports to support the ATF and two 1.5- to 2-in. ports to support the TFF operation.

3.3 | Dual column chromatography design

Dual chromatography is the simplest and perhaps easiest form of ICB that can be implemented (Angarita et al., 2015). The high-level chromatogram skid design shown in Figure 1 allows flexibility for ICB and batch processing. The system uses two pump sizes. A smaller pump is used for the solution concentrates. Larger pumps are used for the diluent and the load. This design has a large processing range. The overall accurate flow rate range is 0.3 to 13 L/min. Although these skids are used by many for all three chromatography steps, the Protein A capture step determines the productivity and timing of the process.

High productivity processes use solution concentrates and dilute with water. The largest processing possible on this system is two 25 L columns with a 10 cm bed depth operated in series, allowing for 57.6 kg/day. The smallest mass that can be processed uses only the smaller pump with no dilution at the lowest accurate flow rate, allowing the use of a 0.6 L column. This set up processes as little as 36 g/day. Two columns operated in parallel (a standard batch operation) can process only as much as 48 kg/day, due to the decreased effective capacity of the column. Because these columns are never operated in series, they can be 20 cm in length, and 50 L each. A one-column capture step can also be considered (Kamga et al., 2018). It would allow only about 24 kg/day production on a 43 L column (data not shown) and can support significantly less bioreactor volume. This mass is less than half of that for the dual column system for about the same Protein A volume. Since these last two options do not overload the Protein A column and run a second column in series to capture the product that flows through the column, they are different from a regulatory perspective than the dual-column chromatography operation. They would likely require a different process characterization and process performance qualification package.

The downstream process can adjust the mass throughput in two ways. Firstly, the capture columns can be underloaded. The load range of the Protein A is assumed to be 10–72 g/L. The second is that the columns can be cycled as few as once per day, to about 15 times each per day, depending upon the titer. The lower limit is set, in part, by the bioburden control strategy, in that we prefer to load a column less than 12 h before sanitizing it. The total in-batch range of productivity is therefore over 200-fold. Between batches, the columns can be changed in size from 0.6 to 25 L. Thus, the overall batch-to-batch productivity range for the downstream is an astonishing 9000-fold range. The polishing steps can be operated in a similar cadence.

The average number of cycles per day is set to avoid changing columns during the 20-day run for commercial processes. Each Protein A column is cycled on average 10 times per day, for a total cycling of 200 cycles per lot. The polishing steps are cycled 12.5 times per day for the maximum productivity, for a total cycling of 250 cycles per lot. While column lifetime may vary from product to product, targeting 200 for the Protein A step and 250 cycles for the polishing steps is not overly burdensome for commercial processes. Poorer column lifetime will require larger columns and fewer cycles per day, or changing the columns during the lot.

The framework also recommends ultraviolet (UV) absorbance detection with two path lengths to allow both high and low concentration measurement. Ideally, the UV detector would be linear up to concentrations of 150 g/L, or about 200 AU/cm to capture the maximum concentration of the elution peak. A detector with 0.1 and 1.0 mm path lengths would be sufficient. These detection limits are necessary to enable accurate yield calculations on every cycle. Optionally, the detector would allow a scan of absorbance from 230 to 320 nm. Spectral analysis of column peaks can be used to estimate purity (Brestrich et al., 2014, 2015, 2016). Additional data connections should be available for expanding PAT methods that are not described here. This UV detection system does not exist commercially.

The dual column chromatography skid may not benefit from being single use, depending upon the application. Small lot sizes will have an increased burden on the COGM of the single use assemblies. This burden is less important in clinical manufacturing, where flexibility and change-over time might be more important. This burden is also less important for very large batches, such as those derived from the 4 × 2000 L example.

The dual column system is backward compatible with batch processing. The downstream can process 48kg/day, or from a fed-batch with 24 g/L titer, from each of the four bioreactors if they are harvested on different days. This titer is well in excess of any standard fed batch process.

3.4 | Virus inactivation

The framework virus inactivation step supports both batch and continuous virus inactivation. The skid performs on-line titration of the peak as it elutes from the Protein A step. The acidified peak then goes into a tank for the batch operation or into a plug flow reactor (PFR) for continuous inactivation. At the end of the incubation time, the product stream is neutralized before passing to the next step.

Those processes that use a surge tank before the virus inactivation step will have a homogeneous product stream entering and exiting the PFR. This homogeneity allows for either a volume-based titration, or one based on a closed-loop pH control. Those steps that titrate the peak in-line without a surge tank will require some feed-forward control based on UV. The UV signal from the Protein A skid will require integration with the virus inactivation skid, or the VI skid will require a UV sensor on the inlet.

The flow rate of acid, base, and water required to titrate the product stream will be linear with respect to UV:

$$Q_{\text{acid}} = A_*UV + b,$$

$$Q_{\text{base}} = C_*UV + d,$$

$$Q_{\text{water}} = E_*UV + f,$$

where A , C , and E are proportionality constants related to the amino acid composition of the product, and b , d , and f are offsets largely related to the steady-state buffer concentration. These constants can be easily determined experimentally. The flow rate of water would be required to maintain a constant ionic strength if needed for the subsequent step. Dilution would not be needed if there was a surge tank after the virus inactivation that averages out the ionic strength variation across the peak. Since the titration of the product stream changes with concentration, the overall flow rate changes during the elution. This variability can be accounted for in the PFR volume, as well as the load of the subsequent step, by sizing each to the largest expected flow rate.

3.5 | Depth filtration

High-density fed-batch processes precipitate HCP and other impurities after the low pH virus inactivation process. The particulates are removed typically by a depth filter.

Perfusion based processes do not precipitate with the same frequency or degree as fed-batch processes (data not shown). Even so, the framework process requires the flexibility of adding a depth filter. The depth filter has challenges for continuous processing. There are not many depth filters that arrive sterile or have a low bioburden specification. This means that depth filtration is an opportunity for bioburden to enter the process. Some depth filters can be sanitized with various solutions, hydroxide being the most typical.

Since the depth filter capacity is assumed to be low (200 L/m²), it will require frequent changing. The framework presumes daily changing, largely to avoid bioburden in depth filters that cannot be sanitized. The filter area is proportional to the Protein A column volume, and varies from 0.3 m² for the clinical process to 6 m² for the 500 kg process. While 6 m² is seen commonly in small manufacturing plants, it is best flushed with its own pump system (not shown).

3.6 | Virus retentive filtration (VRF)

Virus filtration provides a robust and scalable solution for viral clearance in biologic manufacturing. The choice of a suitable virus filter is governed by a combination of feed characteristics and process parameters (Bohonak & Zydney, 2005; Bolton & Apostolidis, 2017; Bolton et al., 2005; Rathore et al., 2014; Syedain et al., 2006). Low flow rates, and concomitant pressure, have been reported to reduce viral retention (Strauss et al., 2017). This effect is dependent on factors such as pH, ionic strength, and membrane composition. This loss of retention under continuous operation has, for many, restricted the VRF process to a batch operation. Tables 1 and 2 depict various scenarios for a constant flow-rate VRF process following the second polishing step. As shown in Table 2, the low productivity scenario would necessitate a membrane area of 0.5 m². Each VRF sub-batch is expected to be operated at 24 h intervals. Here, each sub-batch will take roughly 3 h, yielding the final product pool of 277 L at 24 g/L (Table 2). The concomitant adjustments in membrane area and other operating parameters towards changes in capacity and productivity are mentioned in the supplementary information (Table 2 and Supporting Information Table).

3.7 | Ultrafiltration and diafiltration (UF/DF)

The common framework process enables both batch and single-pass (SP) ultrafiltration and diafiltration (UFDF). The framework uses a flexible single-use skid with the same pumps and different flow path to accommodate both operations.

The batch UF/DF step is shown in Figure 1 and involves batch tangential flow filtration (TFF) and a recirculation skid to attain the desired product concentration. The framework process performs a batch UFDF frequently to avoid the need for a large

system. The entire UF/DF process will be split into as many as 20 sub-batches that are expected to be in-sync with the VRF process. A concentration step is operated continuously as the run progresses. Periodically, the concentrated pool is moved to the DF retentate tank where the diafiltration is performed. The material is moved to the final in-process retentate pool where the final UF concentration occurs continuously as the run progresses. Tables 1 and 2, depicts the process parameters and throughput for a typical TFF module. The size of the filters and pumps used is similar across all scales by controlling the frequency of the batch operation. The filter used for the clinical 6 kg DF is 0.2–1 m² and for the commercial 500 kg batch is 0.4–4 m². Each are sub-batched one time and 20 times, respectively.

The volume of DF buffer required for a batch with high productivity can be prohibitively high (Table 2 and SI Table). For the 500 kg batch, the DF buffer volume is 66,000 L, which is 25% of the total downstream solution volume. This issue can be partially mitigated by the use of buffer concentrates or in-line conditioning. Accurate pumps are needed for this final step.

Recently, alternative approaches to overcome shortfalls of the typical UF/DF operation have been reported in the literature. The advent of single-pass tangential flow filtration (SPTFF) membrane filtration modules has made it possible to attain high protein concentration factors in a single-pass while eliminating the need for repeated product recirculation (Jungbauer, 2013). The use of multistage SPTFF cascade for continuous diafiltration of proteins using cocurrent and countercurrent mode have been demonstrated (Arnold et al., 2019; Huter and Strube, 2019; Jabra et al., 2019; Nambiar et al., 2018; Rucker-Pezzini et al., 2018). Table 2 describes and Figure 1 indicates the proposed implementation of the SPTFF modules for an integrated and continuous UF and countercurrent-DF (CC-DF) process, described in the accompanying article. Here, the feed flow to the UF process is adjusted in a way to spread out each VRF sub-batch pool over 24 h. This allows the UF process to be operated uninterrupted over the entire batch. The retentate stream is then directly fed to the three-stage CC-DF cascade eliminating the need for a surge tank. The DF buffer's countercurrent flow results in at least a 40% reduction in buffer usage than batch DF operation, primarily because the CC-DF step operates at a higher product concentration.

A few pumps are mismatched between the UFDF and SP options. Multihead peristaltic pumps can simplify the pump design considerably. The pumps used on the module could use high-flow and low-flow tubing depending upon the application.

Recent reports also successfully demonstrated the use of hollow-fiber dialyzers for buffer exchange (Yehl et al., 2019). The framework skid would also enable the operation of this step, which has the potential of reducing the total DF buffer required by a factor of 8 from the batch-wise UFDF option.

4 | CONCLUSION

The common ICB framework enables the design of equipment flexible enough to process 6–500 kg lot sizes. The design also allows flexibility for some batch operations and is compatible with legacy processes.

This flexible, mostly single-use design has particular relevancy today during the pandemic. While most COVID-19 mAb projects are made in fed-batch right now, converting from fed-batch to ICB is possible. While converting to ICB will not help in the near term, it would allow manufacturing expansion within about two years. Converting to a perfusion bioreactor would be a relatively large change from a regulatory perspective, and would require strong comparability package. The alternative is a capacity crunch and investment in billions of dollars of stainless-steel infrastructure in countries all over the world. The pandemic exemplifies the uncertainty in manufacturing: the antibody manufacturing may be required for many years to come or it may not. In addition, fast development of scalable mAb manufacturing will help in the next pandemic.

The framework ICB allows companies to harmonize their platform around off-the-shelf equipment. Also, it's possible for contract manufacturers to buy equipment that would be backward compatible with batch processes, as well as future compatible for ICB. This flexibility has not been realized to date. Many companies think of ICB processes as a step forward from which there is no turning back. This paper demonstrates that the common framework ICB can be designed, purchased, and installed with an eye toward the future, and yet without worry about the past.

ACKNOWLEDGMENTS

The authors wish to thank the many participants who participated in the discussions and interviews.

CONFLICT OF INTERESTS

The authors are paid employees of their affiliated biopharmaceutical companies. None have received any compensation for the research reported in this article beyond that from their affiliated employer.

AUTHOR CONTRIBUTIONS

Jon Coffman: *Proposed design basis for the common framework.* Jon Coffman, Mark Brower, Joseph Shultz: *Drafted and critical revision of the design basis.* Ujwal Patil: *Drafted and critical revision of the virus inactivation and ultrafiltration/diafiltration design.* Kenneth Bibbo, Robert Forbes, Brian Horowski, Rick Lu, Rajiv Mahajan: *Drafted plant and equipment design.* Brian Horowski: *Drafted and critically reviewed figures.* Steven Rose, Nicholas Guros: *Drafted and critical revision of the bioreactor design basis.* Jon Coffman, Mark Brower, Joseph Shultz, Ujwal Patil, Kenneth Bibbo, Robert Forbes, Brian Horowski, Rick Lu, Rajiv Mahajan, Steven Rose, Nicholas Guros: *Final approval of the version to be published.*

DATA AVAILABILITY STATEMENT

Data openly available in a public repository that does not issue DOIs.

ORCID

Jon Coffman  <https://orcid.org/0000-0002-4716-258X>

Ujwal Patil  <https://orcid.org/0000-0001-6675-7899>

REFERENCES

- Abbate, T., Sbarciog, M., Dewasme, L., & Vande Wouwer, A. (2020). Experimental validation of a cascade control strategy for continuously perfused animal cell cultures. *Processes*, 8, 413.
- Angarita, M., Müller-Späth, T., Baur, D., Lievrouw, R., Lissens, G., & Morbidelli, M. (2015). Twin-column captureSMB: A novel cyclic process for protein A affinity chromatography. *Journal of Chromatography A*, 1389, 85–95.
- Bohonak, D., & Zydney, A. (2005). Compaction and permeability effects with virus filtration membranes. *Journal of Membrane Science*, 254, 71–79.
- Bolton, G., Cabatingan, M., Rubino, M., Lute, S., Brorson, K., & Bailey, M. (2005). Normal-flow virus filtration: Detection and assessment of the endpoint in bio-processing. *Biotechnology and Applied Biochemistry*, 42, 133–142.
- Bolton, G. R., & Apostolidis, A. J. (2017). Mechanistic modeling of the loss of protein sieving due to internal and external fouling of microfilters. *Biotechnology Progress*, 33, 1323–1333.
- Brestrich, N., Briskot, T., Osberghaus, A., & Hubbuch, J. (2014). A tool for selective inline quantification of co-eluting proteins in chromatography using spectral analysis and partial least squares regression. *Biotechnology and Bioengineering*, 111, 1365–1373.
- Brestrich, N., Hahn, T., & Hubbuch, J. (2016). Application of spectral deconvolution and inverse mechanistic modelling as a tool for root cause investigation in protein chromatography. *Journal of Chromatography A*, 1437, 158–167.
- Brestrich, N., Sanden, A., Kraft, A., McCann, K., Bertolini, J., & Hubbuch, J. (2015). Advances in inline quantification of co-eluting proteins in chromatography: Process-data-based model calibration and application towards real-life separation issues. *Biotechnology and Bioengineering*, 112, 1406–1416.
- Clincke, M. F., Molleryd, C., Samani, P. K., Lindskog, E., Faldt, E., Walsh, K., & Chotteau, V. (2013). Very high density of Chinese hamster ovary cells in perfusion by alternating tangential flow or tangential flow filtration in WAVE Bioreactor—Part II: Applications for antibody production and cryopreservation. *Biotechnology Progress*, 29, 768–777.
- Clincke, M. F., Molleryd, C., Zhang, Y., Lindskog, E., Walsh, K., & Chotteau, V. (2013). Very high density of CHO cells in perfusion by ATF or TFF in WAVE bioreactor. Part I. Effect of the cell density on the process. *Biotechnology Progress*, 29, 754–767.
- Coffman, J. (2020). Common framework spreadsheet. https://docs.google.com/spreadsheets/d/1GWc_qEpugR91A4lbRGJYSOTvQOhvLv6U1eSSDQhbQ/edit?usp=sharing
- Coffman, J., Brower, M., Connell-Crowley, L., Deldari, S., Farid, S. S., Horowski, B., Patil, U., Pollard, D., Qadan, M., Rose, S., Schaefer, E., & Shultz, J. (2020). A common framework for integrated and continuous biomanufacturing. *Biotechnology and Bioengineering*, 118, 1735–1749.
- Diekmann, S., Dürr, C., Herrmann, A., Lindner, I., & Jozic, D. (2011). *Single use bioreactors for the clinical production of monoclonal antibodies—A study to analyze the performance of a CHO cell line and the quality of the produced monoclonal antibody*. Paper presented at BMC Proceedings, BioMed Central.
- Dreher, T., Husemann, U., Adams, T., de Wilde, D., & Greller, G. (2014). Design space definition for a stirred single-use bioreactor family from 50 to 2000 L scale. *Engineering in Life Sciences*, 14, 304–310.
- Hafner, M., Yerushalmi, E., Fays, C., Dufresne, E., & van Stolk, C. (2020). *COVID-19 and the cost of vaccine nationalism*. RAND Corporation.
- Jagschies, G. (2020). *Hierarchy of high impact improvements in bio manufacturing*. Paper presented at Workshop on Innovations in Pharmaceutical Manufacturing. National Academies of Science, Washington, DC.
- Jorjani, P., & Ozturk, S. S. (1999). Effects of cell density and temperature on oxygen consumption rate for different mammalian cell lines. *Biotechnology and Bioengineering*, 64, 349–356.
- Kamga, M. H., Cattaneo, M., & Yoon, S. (2018). Integrated continuous biomanufacturing platform with ATF perfusion and one column chromatography operation for optimum resin utilization and productivity. *Preparative Biochemistry and Biotechnology*, 48, 383–390.
- Karakashev, S. I., & Grozdanova, M. V. (2012). Foams and antifoams. *Advances in Colloid and Interface Science*, 176–177, 1–17.
- Kelley, B. (2009). Industrialization of mAb production technology: The bioprocessing industry at a crossroads. *mAbs*, 1, 443–452.
- Kemp, R. B., & Guan, Y. (1997). Heat flux and the calorimetric-respirometric ratio as measures of catabolic flux in mammalian cells. *Thermochimica Acta*, 300, 199–211.
- Le Merdy, S., Cherradi, Y., & Kalashnikov, P. (2017). *Exploration of synthetic depth filtration applied to mammalian cell harvest*. Merck Millipore.
- Moutafchieva, D., Popova, D., Dimitrova, M., & Tchaoushev, S. (2013). Experimental determination of the volumetric mass transfer coefficient. *Journal of Chemical Technology and Metallurgy*, 48, 351–356.
- Ozturk, S. S. (1996). Engineering challenges in high density cell culture systems. *Cytotechnology*, 22, 3–16.
- Pegel, A., Reiser, S., Steurethaler, M., & Klein, S. (2011). Evaluating disposable depth filtration platforms for mAb harvest clarification. *BioProcess International*, 9, 52–56.
- Proulx, P., Groleau, D., & St-Pierre Lemieux, G. (2019). Introduction on foam and its impact in bioreactors. *Canadian Journal of Biotechnology*, 3, 143–157.
- Radoniqi, F., Zhang, H., Bardliving, C. L., Shamlou, P., & Coffman, J. (2018). Computational fluid dynamic modeling of alternating tangential flow filtration for perfusion cell culture. *Biotechnology and Bioengineering*, 115, 2751–2759.
- Rathore, A. S., Kumar, V., Arora, A., Lute, S., Brorson, K., & Shukla, A. (2014). Mechanistic modeling of viral filtration. *Journal of Membrane Science*, 458, 96–103.
- Strauss, D., Goldstein, J., Hongo-Hirasaki, T., Yokoyama, Y., Hiroto, N., Miyabayashi, T., & Vacante, D. (2017). Characterizing the impact of pressure on virus filtration processes and establishing design spaces to ensure effective parvovirus removal. *Biotechnology Progress*, 33, 1294–1302.
- Syedain, Z. H., Bohonak, D. M., & Zydney, A. L. J. (2006). Protein fouling of virus filtration membranes: Effects of membrane orientation and operating conditions. *Biotechnology Progress*, 22, 1163–1169.
- Wang, S., Godfrey, S., Ravikrishnan, J., Lin, H., Vogel, J., & Coffman, J. (2017). Shear contributions to cell culture performance and product recovery in ATF and TFF perfusion systems. *Journal of Biotechnology*, 246, 52–60.
- Wolf, M. K. F., Bielser, J. M., & Morbidelli, M. (2020). *Perfusion cell culture process for biopharmaceuticals*. Cambridge: Cambridge University Press.
- Yehli, C. J., Jabra, M. G., & Zydney, A. L. (2019). Hollow fiber countercurrent dialysis for continuous buffer exchange of high-

value biotherapeutics. *Biotechnology Progress*, 35, e2763. <https://doi.org/10.1002/btpr.2763>

- Zamani, L., Lundqvist, M., Zhang, Y., Aberg, M., Edfors, F., Bidkhorj, G., Lindahl, A., Mie, A., Mardinoglu, A., Field, R., Turner, R., Rockberg, J., & Chotteau, V. (2018). High cell density perfusion culture has a maintained exoproteome and metabolome. *Biotechnology Journal*, 13, e1800036.
- Zhu, M. M., Mollet, M., Hubert, R. S., Kyung, Y. S., & Zhang, G. G. (2017). Industrial production of therapeutic proteins: Cell lines, cell culture, and purification. In J. A. Kent, T. V. Bommaraju, & S. D. Barnicki, (Eds.), *Handbook of industrial chemistry and biotechnology*, (pp. 1639–1669). Cham: Springer International Publishing.

SUPPORTING INFORMATION

Additional Supporting Information may be found online in the supporting information tab for this article.

How to cite this article: Coffman J, Bibbo K, Brower M, et al. (2021). The design basis for the integrated and continuous biomanufacturing framework. *Biotechnology Bioengineering*, 118, 3323–3333. <https://doi.org/10.1002/bit.27697>